Nanoscience and Nanotechnology 2019, 9(1): 29-36
DOI: 10.5923/j.nn.20190901.03

Morphology of Green Synthesized ZnO Nanoparticles Using Low Temperature Hydrothermal Technique from Aqueous *Carica papaya* Extract

Droepenu Eric Kwabena[1,2,*], Asare Ebenezer Aquisman[1,2]

[1]Graduate School of Nuclear and Allied Sciences, University of Ghana, AE 1, Legon-Accra, Ghana
[2]Universiti Malaysia Sarawak, Faculty of Resource Science and Technology, Kota Samarahan, Sarawak State, Malaysia

Abstract Green synthesis of nanoparticles by plant extracts is gaining grounds in the field of nanotechnology. ZnO Nanoparticles (NPs) were successfully synthesized in this study using two different aqueous extract (fresh leaf and fresh stem bark) from *Carica papaya* on the same precursor and alkaline source (Zinc acetate dihydrate and Potassium hydroxide respectively) in a method by Moazzen et al., 2012 with some modifications. Ultraviolet–Visible spectroscopy (UV–Vis), Fourier Transform Infrared Spectroscopy (FT-IR), Energy-Dispersive X-ray analysis (EDX), Transmission Electron Microscope (TEM) and Scanning Electron Microscopy (SEM) were adopted as characterization techniques for the synthesized samples. The report showed that, fabrication of ZnO NPs from the extracts were successful with thin organic materials surrounding the agglomerated particles. The absorption band and wavelength observed at 444 cm^{-1} and 213.9 nm from the FT-IR and AAS respectively indicates the presence of ZnO in the synthesized samples. UV-Vis spectroscopy further confirmed a strong optical property of the ZnO NPs with a strong absorption peaks at around 365 and 370 nm wavelength. The synthesized samples are made up of flower-like or petal-like shapes with average particle size range of 141-168 nm with width 40 nm and length 89 nm.

Keywords *Carica papaya*, Green Synthesis, Zinc oxide nanoparticles, Hydrothermal

1. Introduction

Nanotechnology is one of the most dynamic research areas in science which is emerging as a strategic priority in several industrialized countries. Nanomaterials, with their nanometric dimensions and varied morphologies, have various applications in different fields such as Pharmaceuticals, Environmental, and Telecommunication [1–4]. Novel materials and devices manufactured using nanotechnology have applications in areas such as health, cosmetics, consumer goods, environmental health, mechanics, optics, biomedical sciences, chemical industries, electronics, space industries, drug-gene delivery and energy science. Others also include optoelectronics, catalysis, single electron transistors, water purification and photoelectrochemical applications [5–7].

More focus is currently on nano-sized semiconductors because of their outstanding properties which have applications in optoelectronic. The versatility of ZnO NPs as semiconductors shows significant optical transparency and luminescent properties in UV–Visible (UV–Vis) regions [8]. Due to their chemical and thermal stability properties, they of great significance in recent years [9]. Various routes for ZnO NPs synthesis have been developed. Some of which include Wet chemical route [10–12], Vapour phase process [13], Hydrothermal [14], Sonochemical [15] and Sol–gel. The rest are Spray pyrolysis, Microwave-assisted techniques, Chemical Vapour Deposition, Ultrasonic condition and precipitation methods [16–21]. These methods of synthesis demand high amount of energy and also involves noxious and harmful chemicals, which may lead to biological risks.

Contrary to chemical route of synthesis, green synthesis of nanoparticles especially ZnO NPs, is attracting much attention due to its excellent characteristic [22]. According to Mahanty *et al.*, [23], the use of green synthesized nanoparticles which are eco-friendly are been utilised as a substitute to the chemically synthesized ones to help control chemical toxicity in the environment. Using plant materials to fabricate nanoparticles results in better defined sizes and morphology as compared to other physicochemical methods [24]. Plant extracts used for the synthesis of nanoparticles are more advantageous than chemical synthesis because, the plant materials act as both reducing and also capping agents

* Corresponding author:
kobladodzie01@yahoo.com (Droepenu Eric Kwabena)
Published online at http://journal.sapub.org/nn

[25–29] which often help to reduce agglomeration of NPs. This helps to control the morphology and as well help to stabilize the NPs.

The rate of nanoparticle growth depends mostly on the concentration of metal ions, amount of plant extract, pH and temperature [30]. Vilchis-Nestor *et al*. [31] investigated the size, morphology, and optical properties of Au NPs and Ag nanostructures using green tea (*Camellia sinensis*) extract in aqueous solution at ambient conditions. They reported that the metal ion concentration and plant extract are controlling factors. They further reported that increasing the amount of *C. sinensis* extract resulted in the nanoparticles been slightly bigger and more spherical. In another study where *Cinnamon zeylanicum* back extract was used, it was realised that, smaller metallic nanoparticles and narrow size distribution occur when more plant extract is added in the reaction medium. The increase in dosage of the extract increases the number of particles as a result of the variation in the number of reductive biomolecules [32]. Different plant extracts have been used in several studies including *Cassia fistula*, *Trifolium pratenese*, *Ocimum basilicum* and so on [33–37].

This study evaluates the effect of aqueous extracts of *Carica papaya* from its fresh leaf and stem bark on the particle size and morphology of ZnO NPs in a hydrothermal procedure by Moazzen et al. [38] with modifications. The morphological features of the synthesized ZnO NPs have been confirmed by using SEM, and TEM techniques. EDX, UV-Vis, FT-IR and AAS were used to analyse the purity of the synthesized materials.

2. Materials and Methods

2.1. Preparation of Plant Extracts

Fresh Leaves and stem bark of *Carica papaya* were cut into pieces and washed under running tap and double distilled water. A weighed mass of 10.0 ± 0.1 g of each material was subjected to 20 minutes boiling in 100 ml of deionized water at 60℃, until the solution changes to light yellow. The extracts were cooled at room temperature, filtered using Smith filter paper (102 Qualitative Ø 125 mm) and stored in schott bottle for further experiments.

2.2. Synthesis of ZnO Nanoparticles

The ZnO particles were prepared as per Moazzen et al, [38] procedure but with some modifications. A weighed mass of 9.15 ± 0.1 g (0.05 mol) of $ZnCH_3COO)_2{\cdot}2H_2O$ was dissolved in 50 ml of deionized water in a 250 ml Schott bottle and heated under 60 ± 2℃ with constant stirring. Also, a weighed mass of 2.80 ± 0.1 g of KOH was dissolved in 25 ml of deionized water in a 100 ml Schott bottle under the same condition as the $Zn(CH_3COO)_2{\cdot}2H_2O$. After both solutions have dissolved completely, the KOH solution was drained from a burette into the $Zn(CH_3COO)_2 \cdot 2H_2O$ solution slowly at 60 ± 2℃ temperature with vigorous stirring for an hour until white precipitate of zinc oxide was formed. A measured volume of 50 ml plant (fresh leaf and bark stem) extract from a burette was allow to drain dropwise into each mixture separately under constant stirring but now under a temperature of 20 ± 2℃ with a magnetic stirrer for 3 hours. The solutions were allowed to cool at room temperature where the precipitate was separated from the supernatant by centrifuging at 4000 rpm for 30 minutes using. The solid zinc oxide precipitate was thoroughly washed and dried under hot air and preserved in air-tight container for characterization.

2.3. Characterization of ZnO Nanoparticles

Different techniques were used to characterize the bio-synthesized ZnO NPs.

2.3.1. UV–Vis Spectra Analysis

The optical property of the sample was determined by measuring its maximum absorbance using UV–Vis spectrophotometry (UV-1800 SHIMADZU). The NPs was dispersed in 95% Absolute ethanol and the absorbance analysed in the range of 300–400 nm.

2.3.2. Scanning Electron Microscopy (SEM)

The morphology of ZnO NPs was determined using scanning electron microscopy (SU3500, Hitachi) with acceleration voltage of 10.0 kV, working distance of 11.6 mm and a pressure of 40 Pa. The powdered solid ZnO NPs were coated on an aluminium plate with the help of adhesive membrane on the aluminium plate.

2.3.3. Transmission Electron Microscope (TEM)

The morphological features especially the size and shape of ZnO NPs was determined using TEM (JOEL 1230, Japan). Basically, copper grid was prepared by applying fomvar coating on the copper grid. ZnO NPs were diluted with ethanol and sonicated with ultrasonic cleaner (Elma, Germany) for 30 minutes. Then, 4 µl of ZnO NPs sample was loaded onto the coated copper grid before being observed under TEM.

2.3.4. Fourier Transform Infra-Red Spectroscopy (FT-IR)

Fourier transform infrared spectroscopy (FT-IR) was used in order to obtain the surface functional group that was present in the ZnO NPs. The characterization involve ZnO NPs powder mixed with Potassium bromide (KBr) in the ratio of 1: 19 [39(Yang et al., 2009). The sample was then placed in the metal hole, pressed until the sample compressed inside the hole, and analysed using FT-IR (Thermo scientifc Nicolet iS10, US). The spectral range of 4000–400 cm^{-1} with the resolution of 4 cm^{-1} was used.

2.3.5. Energy-dispersive X-ray Spectroscopy (EDX)

The purity of the ZnO NPs was determined with EDX (JOEL 6390LA, Japan). The ZnO NPs were diluted with ethanol and sonicated with ultrasonic cleaner (Elma, Germany) for 30 minutes. Then, 4 µl of ZnO NPs sample was loaded onto an aluminium plate before being analysed with the EDX.

2.3.6. Atomic Absorption Spectroscopy (AAS)

To confirm the purity of the samples fabricated by EDX, this technique was employed. A known concentration of the sample was prepared and analysed for the presence of the Zinc element using AAS (iCE 3000 Series AA, Thermo Scientific). Air-acetylene was used as fuel at approximately 2300℃ and flowed at 0.9 L/min. Doubled-beam optics with monochromator reduced the detection limits and provided higher accuracy. The various parameters used in the analysis are in table 1 below;

Parameter	Characteristics
Wavelength (nm)	213.9
Flame type	Air-C_2H_2
Nebulizer uptake (s)	4
Burner height (mm)	14.2
Lamp current (%)	75
Rescale limit (%)	10
Standards (mg/L)	0.3000, 0.6000 and 1.000
Acceptable fit	0.995
Detection limit (mg/L)	0.0033

3. Results and Discussion

3.1. Morphological Analysis (SEM and TEM)

ZnO NPs were analysed using SEM and TEM techniques for their shape and size as illustrated in figure 1.0 (a-d).

From the images, flake-like or petal-like shapes from SEM (Fig 1a & 1b) were recorded which corresponds to a study by Gopal and Kamila [40]. Although a greater proportion of the particles were agglomerated indicating an even distribution of the plant extract in solution, a few were dispersed. The average particle size of the synthesized ZnO nanoparticles ranged between 114-168 nm with the width and length of the petal-like structures been 40 nm and 89 nm respectively. Similar structures were reported in some studies when biological materials such as bacterial strains like *B. lichennoformis* and *Serratia ureilytica*, (HM475278), algae (*Chlamydomonas reinhardtii*), aqueous extract from *Azadirachta indica* were used [41-44].

TEM images (fig 1c & 1d) shows the ZnO NPs agglomerated with a layer of organic materials from the plant extract which serves as a capping agent. These organic materials are also believed to improve the biological potential of NPs when used in drug delivery. Organic materials (phenolic compounds, terpenoids or proteins) surrounding the NPs ensuring stability of the synthesized ZnO NPs could be due to the interaction between the free amino and carboxylic group and the zinc surface [45]. Bonds such as –CO–C–, –C–O– and –C=C– from heterocyclic compounds and amide group from proteins present in the leaf extract forms the capping ligands of the nanoparticle [46-48].

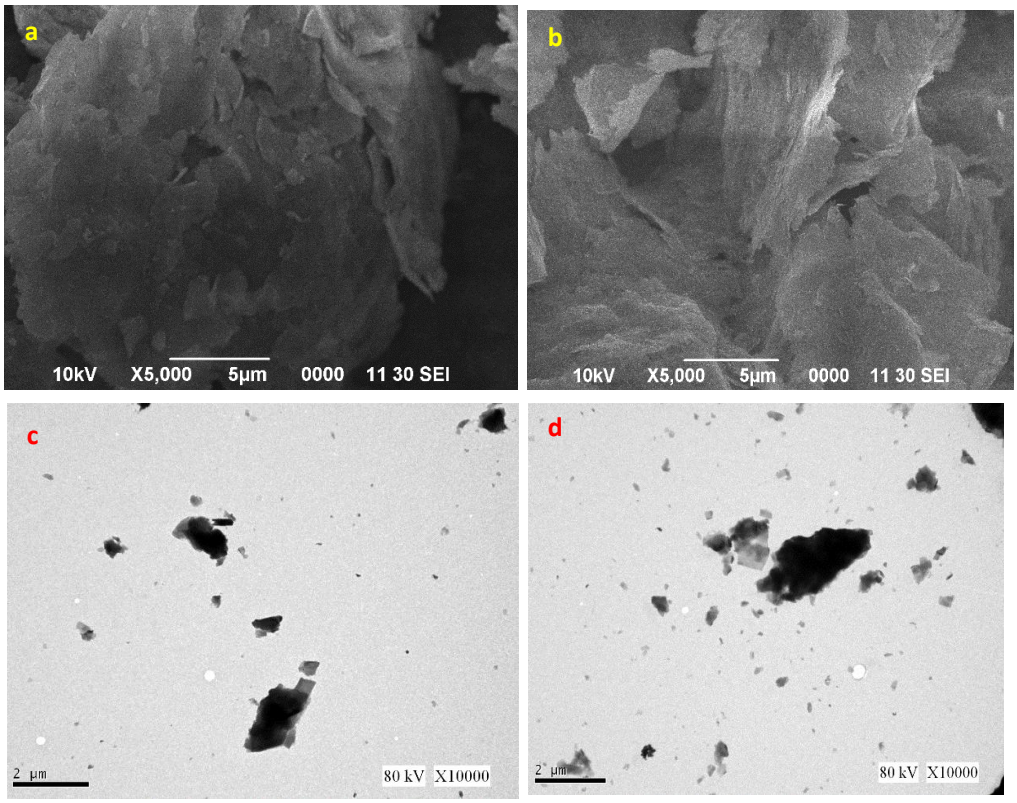

Figure 1. SEM images of ZnO NPs from (a) fresh leaf (b) fresh stem bark. TEM images of ZnO NPs from (c) fresh leaf (d) fresh stem bark aqueous extracts from *Carica papaya*

3.2. UV-Vis Spectroscopy

Determination of the optical properties of the synthesized samples was carried out using Ultraviolet and visible absorption spectroscopy (UV-1800 SHIMADZU UV Spectrophotometer) in the range of 300–400 nm. The absorption spectrum of the bio-synthesized ZnO NPs for the two extracts are illustrated in Figure 2a & 2b.

The optical absorption exhibits strong absorption peaks in UV region at 365.20 and 369.90 nm respectively of the electromagnetic spectrum by the ZnO NPs of both samples. The absorption peak for both samples was attributed to the intrinsic band-gap of Zn-O absorption which confirms the properties of ZnO NPs, known for UV protections in sunscreen products [49,50].

Similar absorption bands recorded for bio-synthesized ZnO NPs in the range of 360-380 nm in previous researches include Ramin et al., Yuhong et al., Huzaifa et al., Vinay Sharma, Santhoshkumar et al., Shubhangi et al. [51-56]. In the case of Shubhangi et al. [56], 391 nm and 402 nm were however recorded for absorption peaks for ZnO NPs synthesized with pectin capping for two different precursors (Zinc nitrate and Zinc acetate). Conversely, Gowsalya et al., Rajesh et al. and Shabnam et al. recorded lower absorption peaks of 295 nm, 330 nm and 350 nm respectively for similar biosynthesis of ZnO NPs [57–59].

Contrary to biosynthesis, chemical route of synthesizing ZnO NPs also gave a high absorption bands ranging from 355 to 380 nm by some studies including; Talam et al., Zak et al., Bian et al., Wang et al., Lavand and Malghe, Akhil and Khan, [60–65]. This indicates that, despite the route used in the fabrication, similar optical properties can be obtained.

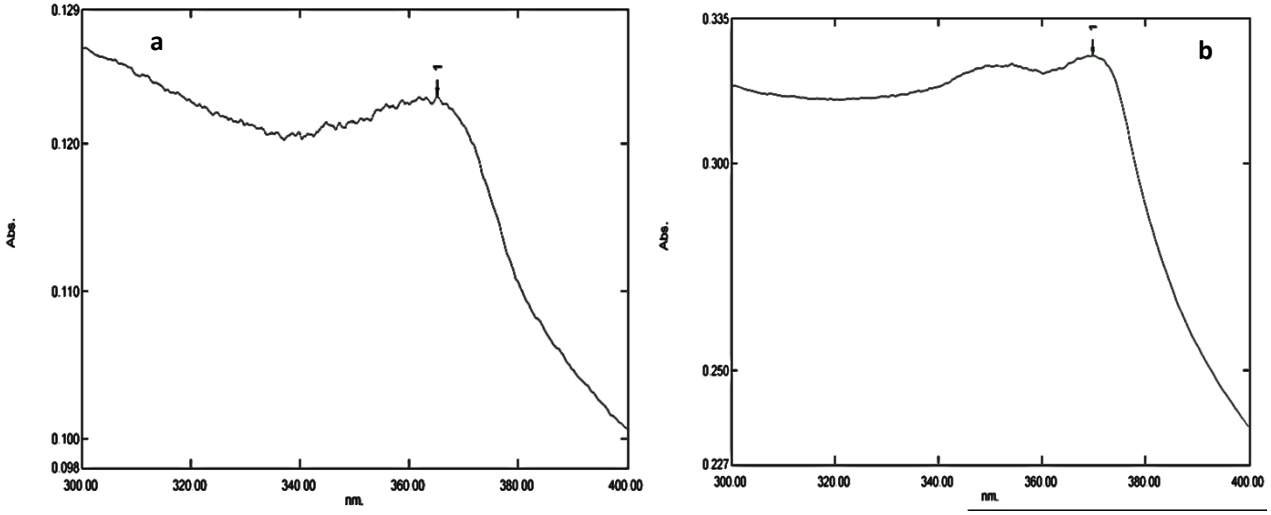

Figure 2. UV-Vis spectrum for ZnO NPs from (a) Fresh leave (b) Fresh stem bark extracts

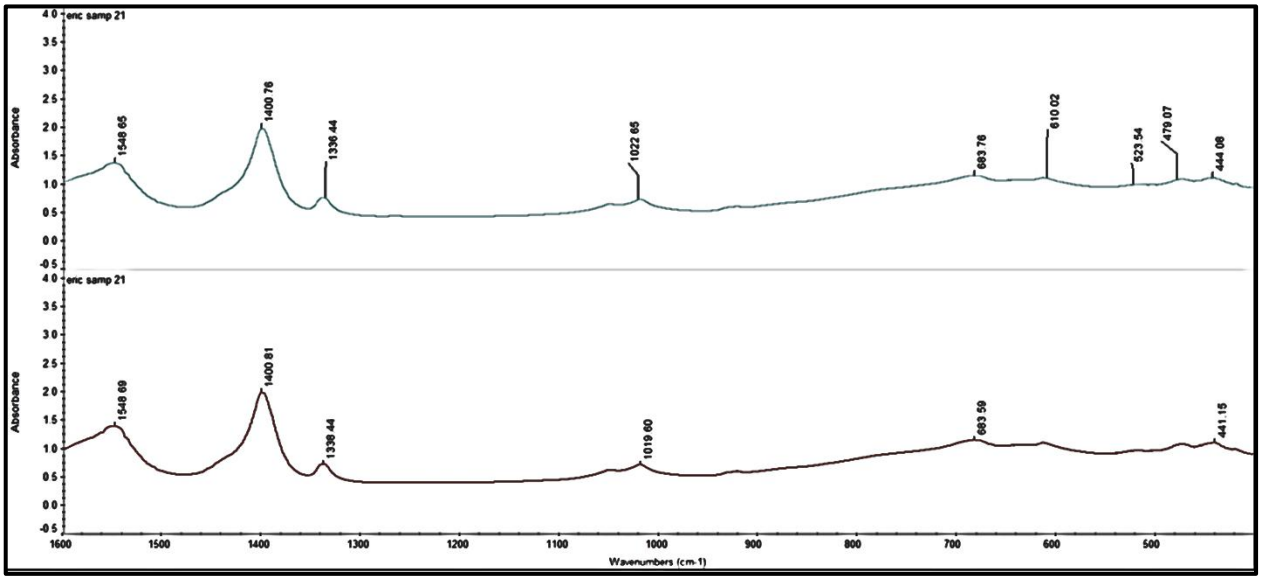

Figure 3. FT-IR spectra of synthesized ZnO NP using *Carica papaya* fresh leaf extract and fresh stem-bark extract

3.3. Surface Functional Groups (FT-IR) Analysis

In determining the functional groups in the synthesized samples, FT-IR (Thermo Scientific, Nicolet iS10) was used in the range of 400–4000 cm^{-1} and the spectra for the two samples are shown in Figure 3.

The two spectra showed broad absorption peaks at 3474.38 and 3474 cm^{-1} representing -OH stretching vibrations [51] for fresh leaf and fresh stem-bark extracts respectively. The Peaks around 1400.76-1633.05 for the prepared samples corresponds to C = C stretch in aromatic rings whereas N-H bending and stretching bonds lie within the peaks of 1629.16 and 3336.94 [52]. Weak peaks obtained for ZnO NPs from fresh leaf extracts at 1022.65 and 1080.21 reveal the presence of C–O and C–N stretching in alcohol and ester respectively whereas 683.76 indicates the presence of C–H bending in alkene. On the other hand, ZnO NPs from fresh stem bark extract gave peak values of 1019.60, 1080.46 and 683.59 denoting the presence of C-O (alcohol), C-N (ester) and C-H (alkene) respectively [51,66]. Similar spectra have been recorded by Gowsalya et al. and Santhoshkumar et al, in their quest in synthesizing ZnO NPs from *Thespesia populnea* and *Passiflora caerulea* leaves respectively [57,55].

From these two results, it can be concluded that, constituents in both samples are similar with peaks obtained between 523.54-683.76 demonstrating the probable presence of C- Alkyl halide. The absorption band observed at 444.08 and 441.75 cm^{-1} for fresh leaf and fresh back respectively are attributed to Zn-O stretching vibrations. In previous studies regarding ZnO NPs they were also able to observe FT-IR spectrum with the band around 400 cm^{-1} [61,39,64,67].

3.4. EDX and AAS Results

The purity or elemental composition of the prepared samples were subjected to EDX and AAS analysis. According to the EDX spectra of the two samples (fig 4a & 4b), no characteristic peaks of any other elements apart from Zn, O and C, were observed, indicating the essential constituents of the fabricated samples. The maximum peak is directly related to Zn indicating a high purity of the synthesized samples.

The Atomic weight percentages of Zn, O and C in the sample from ZnAc and $ZnCl_2$ recorded by the EDX spectra were 49.66%, 3.22%, 47.12%, and 45.13%, 2.02%, and 52.85% respectively. Traces of Chlorine atoms were found in sample 4(b) as impurities. On the other hand, the calculated percentage weight of Zn in the analysed samples using AAS was 47.8% and 54.6% respectively for the two samples.

Similar findings from previous studies by Dobruks and Dugaszewska, [34], reported three peaks recorded by SEM-EDS analysis where the maximum peak indicated Zn.

Thus, the EDX result corroborated with that of the FT-IR where carbon-carbon single and double bonds were revealed in the peaks. The different organic components in the extract forming the thin film on the surface of the ZnO NPs could be attributed to the presence of elemental C in the spectra of the samples [67]. The AAS detected elemental Zinc at 213.9 nm wavelength indicating the presence of the ZnO in the fabricated NPs.

4. Conclusions

The results from this study suggests that, aqueous extracts from fresh *Carica papaya* leaves and stem bark could be used in fabricating ZnO NPs successfully using low temperature hydrothermal technique. The synthesized NPs are pure and agglomerated with average particle size of 141-168 nm with the width and length of the petal-like structures been 40 nm and 89 nm respectively confirmed by SEM characterization. TEM reveals the particles to be agglomerated whereas EDX and AAS indicated a pure ZnO NPs been fabricated. FT-IR spectrum showed the presence of ZnO NPs at band peaks at 444 cm^{-1} for the two samples whereas the optical property assessed by UV- vis gave a strong absorption peak at 365 nm and 370 nm respectively for the two samples. Therefore, the hydrothermal technique employed in this study is one of the most effective methods to obtain a better quality of ZnO NPs.

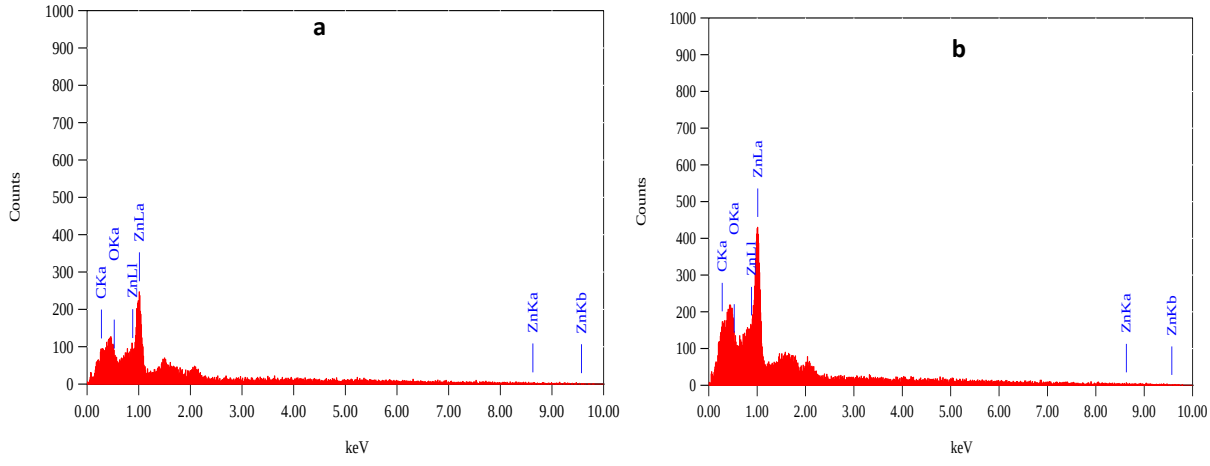

Figure 4. EDX spectra of synthesized ZnO NP using Carica papaya (a) fresh leaf extract and (b) fresh stem-bark extract

REFERENCES

[1] Xu, L. Xing, R. Song, J. Xu, W. and Song, H. (2013). ZnO-SnO_2 nanotubes surface engineered by Ag nanoparticles; synthesis, characterization and highly enhanced HCHO gas sensing properties. J. Meter. Chem. C 1, 2174-2182.

[2] Das, P. Sarmah, K. Hussain, N. Pratihar, S. Das, S. Bhattacharyya, P. Patil, S.A. Kim, H.-S. Iqbal, M. Khazie, A. and Bhattacharyya, S.S. (2016). Novel synthesis of an iron oxalate capped iron oxide nanomaterial; a unique soil conditioner and slow release eco-friendly source of iron sustenance in plants. RSC Adv. 6, 103012-103025.

[3] Sarmah, K. and Pratihar, S. (2017). Synthesis, characterization and photocatalytic application of iron oxalate capped Fe, Fe-Cu, Fe-Co, and Fe-Mn oxide nanomaterial. ACS Sustain. Chem. Eng. 5(1), 310-324.

[4] Bosi, S. Da Ros, T. Spalluto, G. and Prato, M. (2003). Fullerene derivatives; an attractive tool for biological applications. Eur. J. Med. Chem. 38, 913-923.

[5] Colvin, V.L.S. M.C. and Alivisatos, A. (1994). Light emitting diodes made from cadmium selenide nanocrystals and a semiconducting polymer.". Nature, 370: 354-357.

[6] Wang, Y. and H.N. (1991). Nanometer-sized semiconductor clusters: materials synthesis, quantum size effects, and photophysical properties.". J Phys Chem, 95: 525-532.

[7] Naahidi, S. Jafari, M. Edalat, F. Raymond, K. Khademhosseini, A. and Chen, P. (2013). Biocompatibility of engineered nanoparticles for drug delivery. J. Control. Rel. 166, 182- 194.

[8] Cao, B. Liu, R. Huang, Z.X. and Ge, S. (2011). Mater. Lett. 65, 160.

[9] Nunes, J.P. Fernandes, B. Fertunato, E. Vilarinho, P. and Martins, R. (1999). Thin Solid Films. 337, 176–179.

[10] Hu, S.-H. Chen, Y.-C. Hwang, C.-C. Peng, C.-H. and Gong, D.-C. (2010). J. Alloy. Comp. 500 (2), L17–L21.

[11] Wang, A. Ng, H.P. Xu, Y. Li, Y. Zheng, Y. Yu, J. Han, F. Peng, F. and Fu, L. (2014). J. Nanomater. Article ID 451232.

[12] Chen, Y. Zhang, C. Huang, W. Situ, Y. and Huang, H. (2015). Mater. Lett. 141, 294–297.

[13] Chao, L.-C. Chiang, P.-C. Yang, S.-H. Huang, J.-W. Liau, C.-C. Chen, J.-S. and Su, C.-Y. (2006). Appl. Phys. Lett. 88 (25), Article ID 251111.

[14] Tien, H.N. Luan, V.H. Hoa, L.T. Khoa, N.T. Hahn, S.H. Chung, J.S. Shin, E.W. and Hur, S.H. (2013). Chem. Eng. J. 229, 126–133.

[15] Khorsand, Z.A. Majid, W.H.A. Wang, H.Z. Yousefi, R. Moradi, G.A. and Ren, Z.F. (2013). Ultrason. Sonochem. 20 (1), 395–400.

[16] Omri, K. Najeh, I. Dhahri, R. El Ghoul, J. and Elmir, L. (2014). Microelectron. Eng. 128, 53–58.

[17] Zak, A.K. Abrishami, M.E. Majidi, W.H. Abd Yosefi, R. and Hosseini, S.M. (2011). Ceram. Inter. 37, 393–398.

[18] Wu, Y.L. and Liu, S.C. (2002). Adv. Mater. 14, 215–218.

[19] Wei, Y.L. and Chang, P.C. (2008). J. Phys. Chem. Solids. 69, 688–692.

[20] Wang, Y. Zhang, C. Bi, S. and Luo, G. (2010). Powder Technol. 202, 130–136.

[21] Moharram, A.H. Mansour, S.A. Hussein, M.A. and Rashad, M. (2014). J. Nanomater. 1–5.

[22] Gunalan, S. Sivaraj, R. and Rajendran, V. (2012). Green synthesized ZnO nanoparticles against bacterial and fungal pathogens. Prog. Nat. Sci. Mater. Int. 22 (6), 693–700.

[23] Mahanty, A. Mishra, S. Bosu, R. Maurya, U.K. Netam, S.P. Sarkar, B. (2013). Phytoextracts-synthesized silver nanoparticles inhibit bacterial fish pathogen Aeromonas hydrophila. Indian J. Microbiol. 53 (4), 438–446.

[24] Raveendran, P. Fu, J. and Wallen, S.L. (2003). J. Am. Chem. Soc. 125, 13940–13941.

[25] Smitha, S.L. Philip, D. and Gopchandran, K.G. (2009). Green synthesis of gold nanoparticles using Cinnamomum zeylanicum leaf broth. Spectrochimica Acta Part A: Molecular and Biomolecular Spectroscopy. 74(3):735-9.

[26] Bhainsa, K.C. and D'Souza, S.F. (2006). Extracellular biosynthesis of silver nanoparticles using the fungus Aspergillus fumigatus. Colloids and Surfaces B: Biointerfaces. 47(2): 160- 4.

[27] Ahmad, A. Mukherjee, P. Senapati, S. Mandal, D. Khan, M.I. Kumar, R., et al. (2003). Extracellular biosynthesis of silver nanoparticles using the fungus Fusarium oxysporum. Colloids and Surfaces B: Biointerfaces. 28(4):313-8.

[28] Sorbiun, M. Shayegan, M.E. Ramazani, A. and Taghavi, F.S. (2018). Biosynthesis of Ag, ZnO and bimetallic Ag/ZnO alloy nanoparticles by aqueous extract of oak fruit hull (Jaf) and investigation of photocatalytic activity of ZnO and bimetallic Ag/ZnO for degradation of basic violet 3 dye. J. Mater. Sci: Materials in Electronics. 29(4), 2806-14.

[29] Shayegan, M.E. Sorbiun, M. Ramazani, A. and Taghavi, F.S. (2018). Plant-mediated synthesis of zinc oxide and copper oxide nanoparticles by using ferulago angulata (schlecht) boiss extract and comparison of their photocatalytic degradation of Rhodamine B (RhB) under visible light irradiation. Journal of Materials Science: Materials in Electronics. 29(2):1333-40.

[30] Han, K.N. and Kim, N.S. (2009). Challenges and opportunities in direct write technology using nano-metal particles. KONA Powder and Particle Journal. 27:73-83.

[31] Vilchis-Nestor, A.R. Sánchez-Mendieta, V. Camacho-López, M.A. Gómez-Espinosa, R.M. Camacho-López, M.A. and Arenas Alatorre, J.A. (2008). Solventless synthesis and optical properties of Au and Ag nanoparticles using Camellia sinensis extract. Materials Letters. 62(17): 3103-5.

[32] Sathishkumar, M. Sneha, K. Won, S.W. Cho, C.W. Kim, S. and Yun, Y.S. (2009). Cinnamon zeylanicum bark extract and powder mediated green synthesis of nano- crystalline silver particles and its bactericidal activity. Colloids and Surfaces B: Biointerfaces. 73(2):332-8.

[33] Suresh, D. Nethravathi, P.C. Udayabhanu, H. Rajanaika, H. Nagabhushana, H. and Sharma, S.C. (2015). Mat. Sci. Semicon. Proc. 31, 446–454.

[34] Dobrucks, R. and Dugazewska, J. (2016). Saudi J. Biol. Sci. 23(4), 517–523.

[35] Abdul Salam, H. Sivaraj, R. and Venckatesh, R. (2014). Mater. Lett. 131, 16–18.

[36] Vimala, K. Sundarraj, S. Paulpandi, M. Vengatesan, S. and Kannan, S. (2014). Process Biochem. 49, 160–172.

[37] Bhuyan, T. Mishra, K. Khanuja, M. Prasad, R. and Varma, A. (2015). Mat. Sci. Semicon. Proc. 32, 55–61.

[38] Moazzen, M.A.M. Borghei, S.M. and Taleshi, T. (2012). Change in the morphology of ZnO nanoparticles upon changing the reactant concentration. Appl Nanosci. 3, 295–302.

[39] Yang, K. Lin, D. and Xing, B. (2009). Langmuir, 25, 3571–3576. DOI: 10.1021/la803701b.

[40] Venu Gopal, V.R. and Susmita Kamila. (2017). Effect of temperature on the morphology of ZnO nanoparticles: a comparative study. Appl Nanosci, 7:75–82

[41] Tripathi, R.M. Bhadwal, A.S. Gupta, R.K. Singh, P. Shrivastav, A. and Shrivastav, B.R. (2014). ZnO Nanoflowers: novel biobenic synthesis and enhanced photocatalytic activity. J. Photochem. Photobiol. B Biol. 141, 288-295.

[42] Dhandapani, P. Siddarth, A.S. Kamalasekaran, S. Maruthamuthu, S. and Rajagopal, G. (2014). Bio-approach:ureolytic bacteriamediated synthesis of ZnO Nanocrystals on cotton fabric and evaluation of their antibacterial properties. Carbohydr. Polym. 103, 448-455.

[43] Rao, M.D. and Guatam, P. (2016). Synthesis and characterization of ZnO Nanoflowers using chlamydomonas reinhardtii: a green approach. Environ. Prog. Sustain. Energy. 1-7.

[44] Shankar, S.S. Rai, A. Ahmad, A. and Sastry, M. (2004). Rapid synthesis of Au, Ag, and bimetallic Au core–Ag shell nanoparticles using Neem (Azadirachta indica) leaf broth. Journal of Colloid and interface Science, 275(2): 496–502.

[45] Sangeetha G, Rajeshwari S, Venckatesh R. Green synthesis of zinc oxide nanoparticles by aloe barbadensis miller leaf extract: Structure and optical properties. Materials Research Bulletin. 2011;46(12):2560-6.

[46] Jiale H, Qingbiao L, Daohua S, Yinghua L, Yuanbo S, Xin Y, et al. Biosynthesis of silver and gold nanoparticles by novel sundried Cinnamomum camphora leaf. Nanotechnology. 2007;18(10):105104.

[47] Sastry M, Ahmad A, Khan MI, Kumar R. Biosynthesis of metal nanoparticles using fungi and actinomycete. Current science. 2003;85(2):162-70. 115.

[48] Sanghi R, Verma P. Biomimetic synthesis and characterisation of protein capped silver nanoparticles. Bioresource Technology. 2009;100(1):501-4.

[49] Yung, M.M.N. Mouneyrac, C. and Leung, K.M.Y. (2014). Encyclop. Nano.1–17.

[50] Harding, F. Breast Cancer: Cause, Prevention and Cure. Aylesbury: Tekline Publishing; 2006:83.

[51] Ramin, M.-A. Aziz, H.-Y. Abolfazl, B. Saeid, L.-N. and Asadollah, A. (2018). Enhanced anti-bacterial activities of ZnO nanoparticles and ZnO/CuO nanocomposites synthesized using Vaccinium arctostaphylos L. fruit extract. Artificial cells, Nanomedicine, and Biotechnology. 46 (S1), S1200–S1209.

[52] Yuhong, Z. Li, F. Fuigui, H. Aiwu, W. Wen, C. Jinping, Y. Jun, Y. and Feng, P. (2015). Green biosynthesis and characterization of zinc oxide nanoparticles using Corymbia citriodora leaf extract and their photocatalytic activity", Green Chemistry Letters and Reviews, vol. 8, no. 2, pp. 59-63.

[53] Huzaifa, U. Doga, K. and Nahit, R. (2019). Biosynthesis of zinc oxide nanoparticles using Albizia lebbeck stem bark, and evaluation of its antimicrobial, antioxidant, and cytotoxic activities on human breast cancer cell lines. International Journal of Nanomedicine. 14: 87– 100.

[54] Vinay, Sharma. (2012). Sol-Gel mediated facile synthesis of Zinc-Oxide nanoaggregates, their characterization and antibacterial activity. IOSR Journal of Applied Chemistry (IOSR- JAC) ISSN: 2278-5736. 2(6), 52-55.

[55] Santhoshkumar, J. Venkat, S. and Kumar, S.R. (2017). Synthesis of zinc oxide nanoparticles using plant leaf extract against urinary tract infection pathogen. Resource- Efficient Technologies, 3, 459-465.

[56] Shubhangi, M. Priyanka, R. Ashish, W. and Sanjay, M. (2014). Synthesis and comparative study of zinc oxide nanoparticles with and without capping of pectin and its application. World Journal of Pharmacy and Pharmaceutical Sciences. 3(7), 1255-1267.

[57] Gowsalya, V. Santhiya, E. and Kavitha, C. (2017). Synthesis, characterziation of ZnO Nanoparticles from Thespesia populnea. Indian Journal of Applied Research. 7(10), ISSN-2249-555X, IF: 4894, IC Value: 79.96.

[58] Rajesh, K.S. Forishmeeta, B. and Nikahat, P. (2015). Synthesis and Characterization of ZnO Nanoparticles using Leaf Extract of *Camellia sinesis* and Evaluation of their Antimicrobial Efficacy. Int. J. Curr. Microbiol. App. Sci. 4(8): 444-450.

[59] Shabnam, F. Mina, J. and Hassan, K.F. (2019). Green synthesis of zinc oxide nanoparticles: a comparison. Green Chemistry Letters and Reviews. 12(1), 19–24.

[60] Talam, S. Karumuri, S.R. and Gunnam, N. (2012). ISRN Nano, 1–6. DOI: 10.5402/2012/372505.

[61] Zak, A.K. Razali, R. Majid, W.H. and Darroudi, M. (2011). International Journal of Nanomedicine, 6, 1399–1403, DOI: 10.2147/IJN.S19693.

[62] Bian, S.W. Mudunkotuwa, I.A. Rupasinghe, T. and Grassian, V.H. (2011). Langmuir, 27, 6059–6068. DOI: 10.1021/la200570n.

[63] Wang, Y.X. Sun, J. and Yu, X. (2011). In Mater. Sci. Forum, 663, 1103–1106. DOI:10.4028/www.scientific.net/MSF.663-665.1103.

[64] Lavand, A.B. and Malghe, Y.S. (2015). International Journal of Photochemistry, 305–310, DOI: 0.1016/j.jksus.

[65] Akhil, K. Khan, S.S. (2017). J. Photochem. Photobio. B, 167, 136–149. DOI: 10.1016/j.jphotobiol.2016.12.010.

[66] Zhou, L. Lie, Y. Briers, H., et al. (2018). Natural product recovery from bilberry (Vaccinium myrtillus L.) presscake via microwave hydrolysis. ACS Sustain Chem Eng. 6:3676–3685.

[67] Singh, R.P. Shukla, V.K Yadav, R.S Sharma, P.K. Singh, P.K. and Pandey, A.C. (2011). Advance Material Letters, 2, 313–317.

[68] Su Z. (2012). Anthocyanins and flavonoids of Vaccinium L. Pharm Crops. 3:7–37.